High-resolution multidimensional space charge measurement using elastic wave methods

Stéphane Holé*
Laboratoire des Instruments et Systèmes, Université Pierre et Marie Curie, 10, rue Vauquelin, 75005 Paris, France

Jacques Lewiner
Laboratoire d'Électricité Générale, École Supérieure de Physique et de Chimie Industrielles de la Ville de Paris, 10, rue Vauquelin, 75005 Paris, France

(Received 20 November 2000; revised manuscript received 2 April 2001; published 23 August 2001)

In various fields of physics, materials can develop or exhibit a nonuniform space-charge distribution. During the last 20 years various approaches have been proposed for the direct measurement of these distributions involving optical, acoustical, or thermal processes. Most of them, however, lead only to one-dimensional distributions. In this paper we describe two approaches to obtain, in isotropic condensed matter, multidimensional space-charge distributions. They are based on the pressure-wave-propagation method and the electroacoustic method. In the case of the pressure-wave-propagation method, various independent measurements are performed with plane waves at different angles of incidence. A tomographiclike algorithm is then applied to retrieve the multidimensional space-charge distribution. In the case of the electroacoustic method, independent measurements are provided from a set of piezoelectric transducers at various positions. An echographiclike algorithm is then applied to retrieve the multidimensional space-charge distribution. A theoretical model is proposed, and preliminary experimental and simulated results showing the validity of these techniques are presented.

DOI: 10.1103/PhysRevB.64.104106 PACS number(s): 77.22.−d, 72.50.+b, 81.70.Cv

I. INTRODUCTION

In various fields of physics, materials can develop or exhibit a nonuniform space-charge distribution. Such a situation can be found, for instance, in dielectrics stressed by an applied electric field. In this case, this may lead to dramatic effects and eventually to breakdown. In order to understand the phenomena involved and consequently to take the appropriate countermeasures, it has been shown[1] that a nondestructive direct measurement of the space-charge distribution in the material is of great help. Such measurements are carried out with optical, acoustical, and thermal probes. They are generally made with simple structures such as coaxial or plane geometries. However, it has been noticed that many poorly understood phenomena take place in heterogeneous regions. In these regions the electric field, the properties of the insulator, or both have a strong dependence on the position. This is the case, for instance, when the electrodes have irregularities or when the material contains impurities, water trees, or some gradient of chemical structures or physical properties.[2–6]

Different approaches have been proposed in order to measure the space charge in such complex field distributions. In a first approach, a unidimensional technique determines the charge distribution through the sample thickness at a given position on the sample surface after which the position is changed and a new measurement is performed. When the sample surface has been completely scanned, a three-dimensional space-charge distribution can be reconstructed.[6–10] Unfortunately, this technique is slow and due to diffraction the lateral resolution is poor as compared to the resolution in thickness. In another approach, the Kerr effect is used to measure the field distribution in two[11] or three[12] dimensions. This technique gives good results in the case of fluid insulators, but can hardly be applied to diffusive or nontransparent materials.

In this paper we demonstrate that it is possible to obtain the space-charge distribution, in isotropic media, in more than one dimension with an equivalent resolution in any direction by using either of the two different techniques.

One technique relies on the pressure-wave-propagation method. An elastic wave propagating through the sample displaces the trapped charges, which induces a current in a low-impedance-measuring circuit. This current is essentially proportional to the product of the charge amplitude and the displacement integrated over space.[13] In the case of a pulse shaped plane wave, the signal is proportional to the space-charge amplitude integrated over the wave front. Since the same space-charge distribution can be observed from various angles of incidence of the plane wave, a tomographiclike measurement of the charges can be performed. Utilizing a proper algorithm with the tomographiclike measurement makes it possible to retrieve the multidimensional space-charge distribution.

The second technique relies on the electroacoustic method. A variation of the electric field in the insulator produces a modification of the Coulombic force acting on each charge, which in turn acts as the source of elastic waves. Propagating waves proportional to the amplitude of each charge are thus generated at their position.[13] The time for each elastic wave to reach an observation point depends on the location of the initiating charge. The resulting wave amplitude measured at this point at each time is the superposition of the waves radiated from all the sources. In the case of an electric field varying as a short pulse, the wave sources in the sample detected at a given time are those for which the traveling time requested to reach the observation point is the same. By detecting the waves at a range of observation

points, an echographiclike measurement of the space-charge distribution can be made. Again utilizing a proper algorithm, with the resulting amplitude measured at these different points, makes it possible to retrieve the multidimensional space-charge distribution.

It has been shown[2,5,14,15] and theoretically confirmed[13] that charges cannot be considered as the unique source of the signal when the electric field is diverging. Indeed electrostriction may have a contribution comparable in amplitude. As a consequence, the pressure-wave propagation or the electroacoustic methods, applied to diverging-field situations, are not exclusively associated with the charge profile but with the distribution of electrostatic force density. Thus electrostriction must be taken into account in such measurements.

In the next section the expressions for the signals produced by the pressure-wave-propagation method and by the electroacoustic method are briefly reviewed. Section III is devoted to the technique that uses the pressure-wave-propagation method. The signals produced by pressure waves of different angles of incidence are analyzed in the case of plane longitudinal elastic waves. Section IV describes the technique that uses the electroacoustic method. The elastic-wave amplitude at a given position is studied taking into account the radiation diagram of elastic sources. Section V presents a special configuration where only two measurements are necessary to reconstruct simple two-dimensional charge distributions. Some preliminary results that validate the techniques are then shown in the following section.

II. SAMPLE AND SIGNALS

We consider an insulating material containing the charges to be measured and a pair of electrodes. In the case of the pressure-wave-propagation method the electrodes are usually connected through a low-impedance-measuring circuit and the measured signal is the current $i_m(t)$ flowing in that circuit. This signal is produced by a material displacement **u**, which displaces the space charge and modifies locally the dielectric constant. In the case of the electroacoustic method the electrodes are submitted to an extra voltage $V(t)$ in addition to an eventual applied voltage. This extra-voltage modifies the electrostatic force acting on each charge. The signal is measured with a transducer sensitive to the elastic waves created by this variation of force density.

Hereafter, subscripts are used when required to make expressions clearer. Any term is understood to be summed over all values of subscripts that appear twice.

The relations between the variation of the image charges on the electrodes and the material displacement for the pressure-wave-propagation method, and between the elastic sources and the extra voltage for the electroacoustic method have been extensively studied in Ref. 13 for the case of multidimensional distributions. For isotropic solids the signals depend on almost the same parameters whatever the method being used. The first parameter is the electric field **E** in the insulator, which is produced by the charges it contains and by the stress voltage applied to the electrodes. The second parameter is the voltage-normalized electric field $\boldsymbol{\xi}$, which is defined as the field that would exist in the insulator if it were free of charge and if 1 V were applied to the electrodes. This parameter characterizes the system composed of the insulator and of the electrodes. Some other general parameters are also involved, such as the dielectric constant ϵ and the only nonzero coefficients a_{11} and a_{12} of the electrostrictive tensor. The last parameter of influence depends on the method; for the pressure-wave-propagation method it is the material displacement **u** whereas for the electroacoustic method it is the extra voltage $V(t)$.

In order to simplify equation writing, we introduce a linear tensor A_{ij} and a quadratic tensor B_{ij}, both of them derived from Maxwell's tensor. In the case of isotropic solids containing only space charges, one has

$$A_{ij}=\tfrac{1}{2}(2\epsilon+a_{12}-a_{11})(E_i\xi_j+E_j\xi_i)-(\epsilon+a_{12})E_k\xi_k\delta_{ij},$$

$$B_{ij}=(2\epsilon+a_{12}-a_{11})\xi_i\xi_j-(\epsilon+a_{12})\xi_k\xi_k\delta_{ij}. \qquad (1)$$

Here δ_{ij} is Krönecker's symbol, which is equal to 1 if $i=j$ and to 0 otherwise.

In the case of the pressure-wave-propagation method the variation ΔQ of image charge on the electrodes can be obtained by combining Eq. (25) and expression (26) of Ref. 13. Denoting $\mathcal{V}$ as the volume of the insulator, one has

$$\Delta Q=\int_{\mathcal{V}} A_{ij}\frac{\partial u_i}{\partial x_j}dv.$$

The measured current $i_m(t)$, where t is the time, is deduced from this expression by a time differentiation,

$$i_m(t)=\frac{\partial}{\partial t}\int_{\mathcal{V}} A_{ij}\frac{\partial u_i}{\partial x_j}dv. \qquad (2)$$

In the case of the electroacoustic method, the force density f_i, which creates the sources of elastic waves, can be derived from Eqs. (43) and (47) and expression (26) of Ref. 13. One has

$$f_i=\frac{\partial A_{ij}}{\partial x_j}V(t)+\frac{1}{2}\frac{\partial B_{ij}}{\partial x_j}V^2(t). \qquad (3)$$

It can be noticed that the tensor A_{ij} is involved in both the pressure-wave-propagation and the electroacoustic methods. This emphasizes the great similarity of these two methods.

III. TOMOGRAPHY WITH THE PRESSURE-WAVE-PROPAGATION METHOD

The possibility of recovering a multidimensional space-charge distribution with the pressure-wave-propagation method is studied in this section. The principle is to carry out successive measurements with elastic waves at different angles of incidence as is usually performed in tomography.

In the following, we use longitudinal plane waves as is often the case in tomography and in the pressure-wave-propagation method. During the propagation, the material displacement **u** has the same direction **d** as of the wave vector. Moreover, the displacement is identical on any plane

perpendicular to the direction **d** (**d** is a unit vector).

We assume in this section that the medium in which the plane wave is traveling presents no attenuation and no dispersion so that the shape f of the elastic wave is not deformed during the propagation. However the function f must be twice differentiable in order to fulfill the propagation equation. Denoting V_L as the speed of sound of longitudinal waves and **x** as the coordinate of an arbitrary point M in the insulator, the displacement **u** can be written as

$$\mathbf{u}=f(t-\mathbf{d}\cdot\mathbf{x}/V_L)\mathbf{d}. \tag{4}$$

We introduce the second-order derivative $f''(\eta)=d^2f(\eta)/d\eta^2$ of the function $f(\eta)$ where $\eta=t-\mathbf{d}\cdot\mathbf{x}/V_L$. Using the relation $\partial f/\partial x_i=-(d_i/V_L)\partial f/\partial t$ and neglecting the variations of the linear tensor A_{ij} during the measurement, one obtains

$$i_m(t,\mathbf{d})=-\frac{1}{V_L}\int_{\mathcal{V}}A_{ij}d_id_jf''(t-\mathbf{d}\cdot\mathbf{x}/V_L)dv. \tag{5}$$

As expected, the measured current is dependent on the direction **d** of the plane wave. The integration by parts of Eq. (5) can be simplified by extending the domain of integration over the whole space. This can be done directly since the linear tensor is equal to zero outside volume $\mathcal{V}$ due to the fact that the electric field is equal to zero in the electrodes. Noticing that $\partial^2 f/\partial x_i\partial x_j=d_id_jf''/V_L^2$, Eq. (5) can be rewritten as

$$i_m(t,\mathbf{d})=-V_L\int A_{ij}\frac{\partial^2 f(t-\mathbf{d}\cdot\mathbf{x}/V_L)}{\partial x_i\partial x_j}dv. \tag{6}$$

A first integration by parts leads to

$$i_m(t,\mathbf{d})=-V_L\int\frac{\partial(A_{ij}\partial f/\partial x_j)}{\partial x_i}dv+V_L\int\frac{\partial A_{ij}}{\partial x_i}\frac{\partial f}{\partial x_j}dv. \tag{7}$$

The first integral is equal to zero since A_{ij} is zero at infinity (i.e., in the electrodes). A second integration by parts on the remaining integral results in

$$i_m(t,\mathbf{d})=V_L\int\frac{\partial(f\partial A_{ij}/\partial x_i)}{\partial x_j}dv-V_L\int\frac{\partial^2 A_{ij}}{\partial x_i\partial x_j}fdv. \tag{8}$$

For the same reason the first integral is equal to zero and one gets

$$i_m(t,\mathbf{d})=-V_L\int\frac{\partial^2 A_{ij}}{\partial x_i\partial x_j}f(t-\mathbf{d}\cdot\mathbf{x}/V_L)dv. \tag{9}$$

Hence, the spectrum of the measured current $\hat{i}_m(\omega,\mathbf{d})$, where ω denotes the circular frequency and $\iota=\sqrt{-1}$, is

$$\hat{i}_m(\omega,\mathbf{d})=-V_L\hat{f}(\omega)\int\frac{\partial^2 A_{ij}}{\partial x_i\partial x_j}e^{-\iota(\omega\mathbf{d}/V_L)\cdot\mathbf{x}}dv. \tag{10}$$

The integral of Eq. (10) is the space Fourier transform of $\partial^2 A_{ij}/\partial x_i\partial x_j$. It can be seen that $\hat{i}_m(\omega,\mathbf{d})$ is proportional to this space Fourier transform along a line in the reciprocal space defined by a wave vector $\mathbf{k}=\omega\mathbf{d}/V_L$. Consequently $\partial^2 A_{ij}/\partial x_i\partial x_j$ can be retrieved by the inverse transformation

$$\frac{\partial^2 A_{ij}}{\partial x_i\partial x_j}=-\frac{1}{(2\pi)^3V_L}\int\frac{\hat{i}_m(\mathbf{k})}{\hat{f}(\mathbf{k})}e^{\iota\mathbf{k}\cdot\mathbf{x}}d\mathbf{k}^3.$$

Since the unit vector **d** is completely defined by its angular coordinates θ and ϕ in a spherical coordinate system, one has

$$\mathbf{d}=\begin{pmatrix}\sin(\theta)\cos(\phi)\\ \sin(\theta)\sin(\phi)\\ \cos(\theta)\end{pmatrix}, \tag{11}$$

and thus

$$\frac{\partial^2 A_{ij}}{\partial x_i\partial x_j}=-\frac{1}{(2\pi)^3V_L^4}\int_0^{\pi}\int_0^{2\pi}\int_0^{\infty}\frac{\hat{i}_m(\omega,\theta,\phi)}{\hat{f}(\omega)}\times\omega^2\sin(\phi)e^{\iota\mathbf{k}\cdot\mathbf{x}}d\omega\,d\theta\,d\phi. \tag{12}$$

It is also possible, using expression (1) of the linear tensor A_{ij} and denoting $\rho=\partial(\epsilon E_i)/\partial x_i$ as the space-charge density, to obtain at any point in the volume of the insulator another expression for $\partial^2 A_{ij}/\partial x_i\partial x_j$. One has

$$\frac{\partial^2 A_{ij}}{\partial x_i\partial x_j}=\frac{2\epsilon+a_{12}-a_{11}}{2\epsilon}\frac{\partial(\rho\xi_j)}{\partial x_j}-\frac{a_{11}+a_{12}}{2}\frac{\partial^2(E_i\xi_i)}{\partial x_j^2}. \tag{13}$$

Thus using the vectorial operators divergence and Laplacian, the above equation becomes

$$\frac{\partial^2 A_{ij}}{\partial x_i\partial x_j}=\frac{2\epsilon+a_{12}-a_{11}}{2\epsilon}\mathrm{div}(\rho\boldsymbol{\xi})-\frac{a_{11}+a_{12}}{2}\nabla^2(\mathbf{E}\cdot\boldsymbol{\xi}). \tag{14}$$

It can be seen that this expression does not lead directly to the charges but to the divergence of the electrostatic force produced by $\boldsymbol{\xi}$ on these charges. The space-charge distribution can be deduced from this expression by using any known method, for instance, a finite-element method. An example will be shown in Sec. VI B. It can be noticed in Eq. (12) that the Fourier spectrum of the elastic-wave shape $\hat{f}(\omega)$ is needed to extract the charge density in absolute units. The calibration procedure usually used for the pressure-wave-propagation method can be applied.[16] This procedure allows for the connection between signal and charge amplitudes by using any known charges, generally the image charges on the electrodes. If attenuation and dispersion cannot be neglected, it is possible to generalize this analysis by applying the above expressions to each component of the spectrum taking into account the nature of the material and the Fourier spectrum of the wave.

IV. ECHOGRAPHY WITH THE ELECTROACOUSTIC METHOD

The possibility of recovering a multidimensional space-charge distribution with the electroacoustic method is studied in this section. The principle is to carry out a set of measurements at different observation points and to use the traveling times of the waves to determine the position of their sources, as is usually performed in echography.

An elastic wave in a solid is the superposition of a longitudinal wave and two transversal waves. In isotropic solids, these waves are independent and their velocities do not depend on the angle of incidence. The velocity of the longitudinal wave is $V_L=\sqrt{C_{11}/m_v}$ and that of transversal waves is $V_T=\sqrt{(C_{11}-C_{12})/2m_v}$, where C_{11} and C_{12} are the only nonzero coefficients of the elastic stiffness tensor and m_v is the mass density. Since $V_L \geqslant \sqrt{2}V_T$, longitudinal waves always reach a given position before transversal waves. Consequently, it is possible to separate these different modes of propagation by choosing an appropriate time window. This is generally done by coupling a waveguide to the sample with a length sufficient to introduce enough delay between transversal and longitudinal waves for their separation.

The wave equation, which connects space and time variations of the displacement **u** in isotropic solids stressed by a force density **f** is given by

$$m_v\frac{\partial^2\mathbf{u}}{\partial t^2}=\tfrac{1}{2}(C_{11}+C_{12})\mathbf{grad}(\mathrm{div}\ \mathbf{u})+\tfrac{1}{2}(C_{11}-C_{12})\boldsymbol{\nabla}^2(\mathbf{u})+\mathbf{f}. \tag{15}$$

By splitting the material displacement **u** into two vectors, $\mathbf{u}_L$ and $\mathbf{u}_T$ where $\mathbf{curl}(\mathbf{u}_L)=\mathbf{0}$ and $\mathrm{div}(\mathbf{u}_T)=0$, Eq. (15) can be rewritten as

$$\left[m_v\frac{\partial^2\mathbf{u}_L}{\partial t^2}-C_{11}\boldsymbol{\nabla}^2(\mathbf{u}_L)\right]+\left[m_v\frac{\partial^2\mathbf{u}_T}{\partial t^2}-\frac{1}{2}(C_{11}-C_{12})\boldsymbol{\nabla}^2(\mathbf{u}_T)\right]=\mathbf{f}. \tag{16}$$

Taking the divergence of this equation and introducing the deformation $S=\mathrm{div}(\mathbf{u}_L)$, it becomes

$$\frac{\partial^2 S}{\partial t^2}-V_L^2\nabla^2(S)=\frac{1}{m_v}\mathrm{div}(\mathbf{f}). \tag{17}$$

As one can see, Eq. (17) is a standard form of the wave equation in a fluid having a velocity of sound V_L and including the source distribution $\mathrm{div}(\mathbf{f})/m_v$. Therefore the general solution[17] of S at a position M is

$$S(M,t)=\frac{1}{m_v}\int_{\mathcal{V}'}\int_{t'} g(M,M',t-t')\,\mathrm{div}[\mathbf{f}(M',t')]\,dt'\,dv', \tag{18}$$

where $\mathcal{V}'$ represents the entire space, $M'\in\mathcal{V}'$, and t' represents all times. The function $g(M,M',t-t')$ is called the Green's function. In a nonlossy infinite medium $g(M,M',t-t')$ is expressed using the Dirac's function $\delta(t)$ as

$$g(M,M',t-t')=\frac{\delta(t-t'-\|\mathbf{MM}'\|/V_L)}{4\pi V_L^2\|\mathbf{MM}'\|}. \tag{19}$$

Usually, transducers do not produce a signal proportional to the deformation in the medium, but a signal almost proportional to the derivative of the material displacement over the direction of the transducer thickness. Since $S=\mathrm{div}(\mathbf{u}_L)$, it can also be stated that

$$\mathbf{u}_L(M,t)=\frac{1}{m_v}\int_{\mathcal{V}'}\int_{t'}\mathbf{G}(M,M',t-t')\,\mathrm{div}[\mathbf{f}(M',t')]\,dt'\,dv'. \tag{20}$$

Here the Green's function $\mathbf{G}(M,M',t-t')$ is a vector whose divergence is $g(M,M',t-t')$. Since longitudinal waves have a higher sound velocity than transversal waves, and as long as transversal waves have not reached the point of observation M, the longitudinal displacement $\mathbf{u}_L$ can be directly replaced by the total displacement **u**. Introducing the Heaviside's function $H(t)$, $\mathbf{G}(M,M',t-t')$ can be written in a nonlossy infinite medium as

$$\mathbf{G}(M,M',t-t')=-\frac{(t-t')\mathbf{MM}'}{4\pi\|\mathbf{MM}'\|^3}H(t-t'-\|\mathbf{MM}'\|/V_L). \tag{21}$$

Equations (18) and (20) provide the deformation and the longitudinal displacement at any arbitrary time and position. In order to reconstruct the source distribution $\mathrm{div}(\mathbf{f})/m_v$ everywhere in a given volume, these integrals have to be inverted. For this purpose it is necessary to measure S or $\mathbf{u}_L$ on a surface surrounding the sources to ensure the uniqueness of the solution. In this case the three-dimensional space coordinates of the sources are reconstructed from the two-dimensional space coordinates of the surface, where the transducers are positioned, and the one-dimensional time coordinate derived from the measured traveling times.

As in the case of the pressure-wave-propagation method the inverse problem does not yield directly the charge distribution but rather the divergence of the force density. However if the amplitude and the direction of the longitudinal displacement $\mathbf{u}_L$ can be measured, the direction of the force density can also be extracted. As already mentioned in Sec. III the space-charge distribution can be deduced from the divergence of the force density by using any known method, for instance, a finite-element method. The calibration procedure usually used for the electroacoustic method can be applied in order to obtain the space-charge density in absolute units. This procedure allows for the connection between signal and charge amplitudes by using any known charge, generally the image charges on the electrodes.

V. ANAGLYPH IMAGES

Before discussing some preliminary results, we consider the particular case of simple two-dimensional distributions. These distributions can be easily recovered using only two

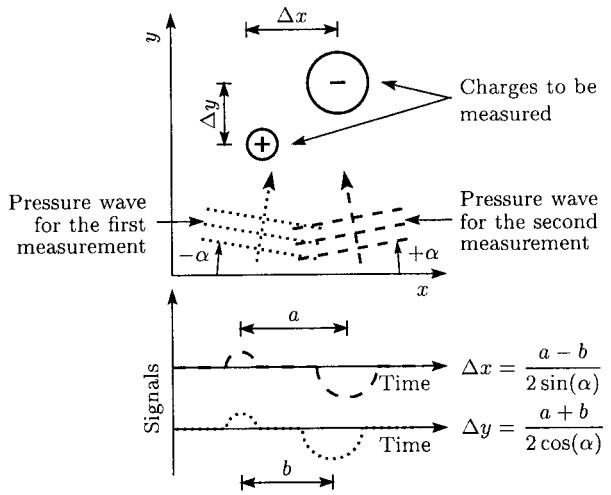

FIG. 1. Determination of a two-dimensional space-charge distribution using two pressure-wave-propagation measurements.

measurements taken at two angles of incidence for the pressure-wave-propagation method or at two positions for the electroacoustic method. Indeed, if the two angles of incidence or the two positions are relatively close to each other, the two measurements are very similar. However the signal produced by a given charge does not appear exactly at the same time in the two measurements but is displaced by a small delay. This delay is directly proportional to the position of the charge along the axis perpendicular to the mean direction of the two waves (pressure-wave-propagation method), or of the two transducers used to carry out the measurements (electroacoustic method). This is illustrated in Fig. 1 where the position of negative charges relative to positive charges is determined. Thus if the delay between the signals corresponding to the same event can be estimated, a two-dimensional image of the charges can be retrieved.

The brain currently performs this job in order to reconstruct a three-dimensional space from measuring the relative distance between the positions of the same object in the two images provided by each eye. Consequently the brain can be used to reconstruct the space-charge distribution by providing two images each representing a measurement, the first for one eye and the second for the other. For instance, the first image can be coded in red to represent the amplitudes of the first measurement and the other in blue to represent the amplitudes of the second measurement. The superposition of these two images is called an anaglyph image. By using vision spectacles having for each eye a different color filter, one gets a three-dimensional image of the charges as in a ''direct'' vision of the charges at different positions. Of course many other techniques are available to present an image to one eye and another image to the other eye, for instance, using diffraction gratings or polarizers.

Unfortunately the estimation of the delay becomes very difficult as the charge distribution becomes more complex, for instance, if at a given time in a measurement the signal is produced by charges distributed at many positions. Since the brain is more accustomed to treat opaque objects rather than semitransparent ones, the reconstruction is not ''naturally'' done by the brain in this particular case.

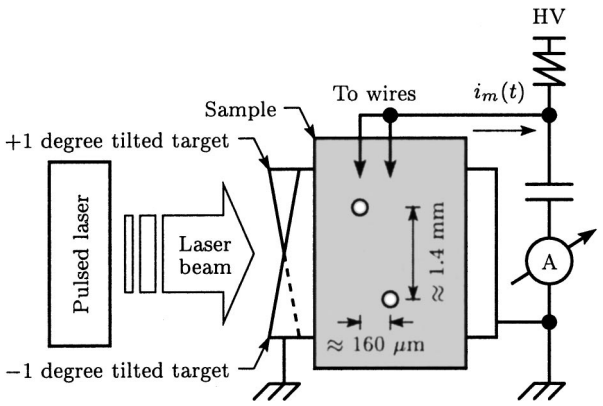

FIG. 2. Experimental setup for the pressure-wave-propagation measurements.

VI. RESULTS AND DISCUSSION

In this section preliminary results are presented in order to validate the concept applied to the above two techniques. Their relative advantages and disadvantages are discussed.

A. Experimental results

The measurements presented in this section were made with epoxy-resin samples delimited by two planar electrodes and including one or two biased wires in order to create a two-dimensional electric field and thus simulate a localized space charge.

Figure 2 illustrates the experimental setup used for the technique based on the pressure-wave-propagation method. A sample including two wires is coupled to an aluminum target. This target is separated in two parts having the same back face. The front face however has two sides slightly tilted with respect to the back face in two opposite directions with an angle of ±1°. Due to Descartes-Snell's law, the pressure pulse created by the impact of a laser pulse enters into the insulator with an angle of ±0.4° depending on which side of the target the laser pulse impinges. The two measurements corresponding to these two angles of incidence are presented in Fig. 3. As expected, the delay between the events due to the wires is different in the two measurements. Since the two angles of incidence are not very different, the first event in the two measurements is due to the same wire, that is to say, the one closer to the target electrode. For the

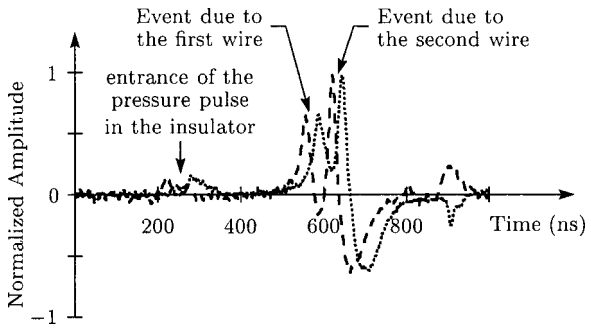

FIG. 3. Pressure-wave-propagation signals produced by pressure pulses having two different angles of incidence.

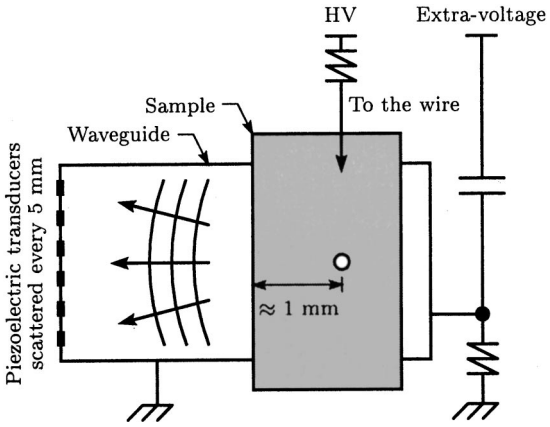

FIG. 4. Experimental setup for the electroacoustic measurements.

same reason the second event in the two measurements is due to the other wire, the one further away from the target electrode. The delay between the two events in the first measurement is 66 ns (about 165 μm) and 58 ns (about 145 μm) in the second. Using the expressions included in Fig. 1, one finds a distance between the wires of 1.43 mm along the lateral direction and 155 μm along the thickness. This result corresponds almost exactly (error of 30 μm along the lateral direction and 5 μm along the thickness) to the dimensions imposed by the mould used to prepare the sample (see Fig. 2). This experiment validates the anaglyph technique and also the tomographic technique using the pressure-wave-propagation method.

Figure 4 illustrates the setup used for the technique based on the electroacoustic method. An epoxy-resin sample including one wire is coupled to an aluminum waveguide on which six transducers are distributed every 5 mm along a line. The events corresponding to the wire are more or less delayed in the measured signal depending on the position of the wire relative to the transducers. Figure 5(a) presents the

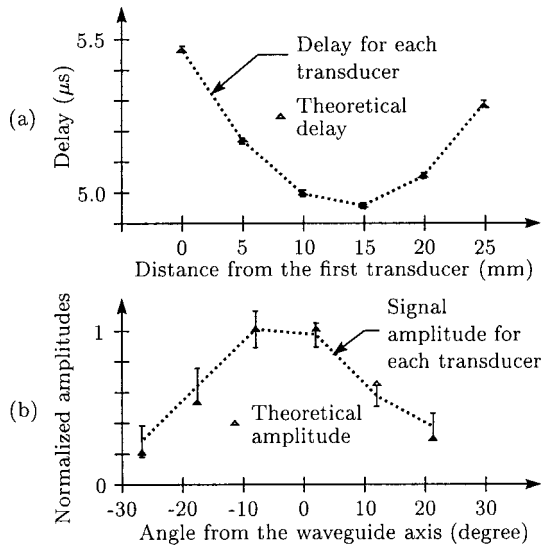

FIG. 5. Experimental and theoretical delays (a) and amplitudes (b) of the event due to the wire in the electroacoustic measurements.

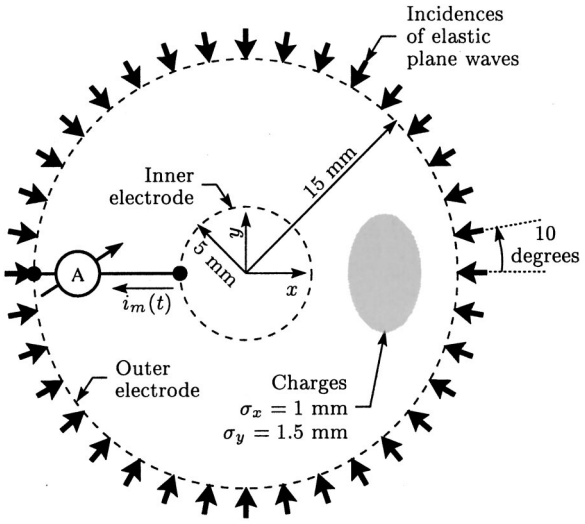

FIG. 6. Configuration and parameters of the polyethylene coaxial sample used for the simulations.

experimental delays of the event due to the wire and the corresponding theoretical delay. This theoretical delay has been calculated with a 30 mm length waveguide and a wire positioned at 1 mm from the sample surface. The amplitude of the signal depends also on the position of the wire. Indeed, the transmission coefficient from the sample to the waveguide and the response of the transducers vary with the angle of incidence of the elastic waves. Figure 5(b) presents both theoretical and experimental amplitudes of the event due to the wire. The theoretical points have been estimated with the parameters previously mentioned and the corresponding ratio of thickness over width for each transducer. Though the transducers have the same thickness, their widths are slightly different making the ratio of thickness to width vary from 0.10 to 0.17. As one can see, the theoretical curves of Fig. 5 fit almost exactly the experimental results and thus validate the echographic technique using the electroacoustic method. The error in the wire position obtained from these measurements is less than 100 μm along the lateral direction and of the order of 8 μm along the thickness. These errors are relatively small owing to the dimension of each transducer (200 μm thick and $\approx 2 \times 2$-mm^2 surface).

B. Simulated results

The signals presented in this section were obtained by a simulation using a finite-element method[14,15] in order to validate the mathematical inverse expression (12) of the technique based on the pressure-wave-propagation method. A polyethylene coaxial sample containing a localized Gaussian space-charge distribution has been considered. The parameters of the sample and of the charge distribution are illustrated in Fig. 6.

A series of 36 signals have been calculated, each deriving from a plane elastic wave propagating in directions located every 10° around the sample. The shape of the plane waves has been determined from a real measurement in which the pulse is broad enough to allow a simulation with a relatively small number of finite elements. Figure 7 shows some of the

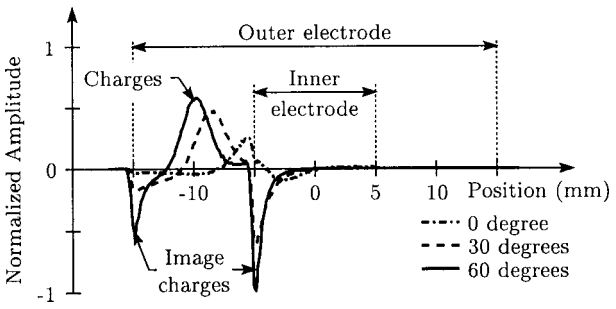

FIG. 7. Examples of calculated signals using a finite-element method and an experimentally determined pressure shape.

signals. The influence of space charges and also of image charges on the electrodes can be seen.

The application of the mathematical inverse expression (12) to the 36 calculated signals leads to the divergence of the force density created by the electric field $\boldsymbol{\xi}$ on the charges. The force density $\rho\boldsymbol{\xi}$, and then the charge density, can be determined solving, for instance, $\mathrm{div}[\mathbf{grad}(a)]=b$ using a finite-element method. In this particular case of Gauss's equation, $\mathbf{grad}(a)$ is the force density to be determined and b is the result of expression (12). Taking a square domain including the insulator with also the electrodes and applying Dirichlet's conditions on the boundary, we obtain the charge distribution presented in Fig. 8. The resulting charge distribution, obtained from the force density and $\boldsymbol{\xi}$, which depends only on the structure, is very similar to the charge distribution assumed for the simulation and is shown in Fig. 6. We also observe the image charge on the electrode (superimposed on the dashed line in Fig. 8). For small amplitude densities, deviations can be observed. This can be attributed to the rather broad profile of the elastic wave used in this case and to the relatively small number of angles of incidence. However this validation of the mathematical inverse expression (12) of the technique based on the pressure-wave-propagation method shows that it is not necessary to have a large number of angles of incidence to lead to a relatively good representation of the real situation.

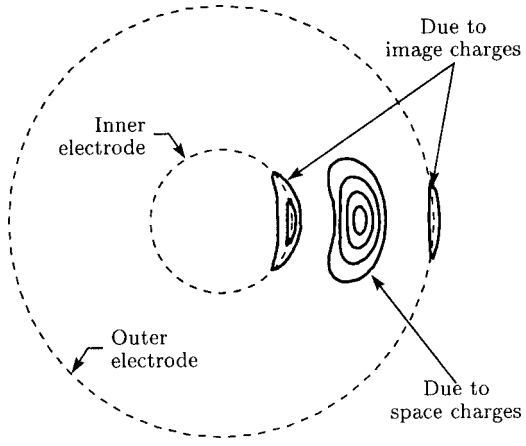

FIG. 8. Charges determined by the tomographic technique. Internal charges are shown with positive level curves whereas image charges are shown with negative level curves.

C. Discussion

The two techniques described in this article lead to the same information: the divergence of the force density rather than the charge distribution. The charge can be deduced by applying, for instance, a finite-element method. However some differences must be pointed out. Because it is based on the pressure-wave-propagation method, the tomographic technique has a large signal-to-noise ratio.[1] Though this technique also takes advantage of the mathematical solution provided by Eq. (12) many angles of incidence are required, which may result in long measuring times. Thus it is particularly well fitted for systems having a slow evolution with time. The echographic technique has a lower signal-to-noise ratio due to two factors: the limited amplitude of the extra voltage and the necessary small size of the transducers that must be used. Of course this ratio can be improved by averaging successive measurements but such an averaging also results in longer times for the measurements. If no averaging is required, high rate measurements can be performed since the signals from all the transducers can be measured at the same time and thus rapid evolution of charges can be followed. Contrarily to the tomographic technique the inverse solution involves complex algorithms. However if both the amplitude and the direction of the displacement can be measured, the amplitude and the direction of the force density can be recovered. This allows the charges and the field in the insulator to be determined with more accuracy.

In the models presented, the effect of attenuation, dispersion, and reflection on boundaries or impedance mismatches have not been taken into account in the theoretical developments. Their effects may lead to non-negligible distortions in the solution if too simple inverse algorithms are used. However, as already stated, attenuation and dispersion can be taken into account by applying the proposed expressions to each component of the spectrum.

VII. CONCLUSION

In this article, two techniques for the multidimensional measurement of space charges have been introduced. The preliminary results fit well the theoretical development proposed. The first technique is based on the pressure-wave-propagation method using elastic plane waves at different angles of incidence. Its advantages are the large signal-to-noise ratio and the simple mathematical inverse expression. Unfortunately it requires a series of measurements taken successively with elastic waves having different angles of incidence and thus a global long time. The second technique is based on the electroacoustic method using receiving transducers at different positions. Its advantage is that a measurement is very fast. Unfortunately, the signal-to-noise ratio may be poor as the transducer surface is reduced. Moreover, there is no simple mathematical inverse expression, which makes the inverse problem more difficult to solve. For two-dimensional simple charge distributions, we have shown that only two measurements are required. The set up is thus sim-

plified and, by the construction of anaglyph images, for instance, the human brain provides the inverse algorithm.

These techniques, which have been validated in simple cases, have a large potential for the study of space-charge buildup in materials with complex field distributions and would lead to high-accuracy measurements. Further developments must now be carried out in order to evaluate the limits of these approaches.

*Electronic address: stephane.hole@espci.fr

[1] T. Mizutani, IEEE Trans. Dielectr. Electr. Insul. **1**, 923 (1994).
[2] T. Ditchi, G. Bazin, J. Lewiner, and C. Alquié, Appl. Phys. Lett. **67**, 1025 (1995).
[3] Y. Zhang, J. Lewiner, C. Alquié, and N. Hampton, IEEE Trans. Dielectr. Electr. Insul. **3**, 778 (1996).
[4] Y. Li, J. Kawai, Y. Ebinuma, Y. Fujiwara, Y. Ohki, Y. Tanaka, and T. Takada, IEEE Trans. Dielectr. Electr. Insul. **4**, 52 (1997).
[5] O. Naz, T. Ditchi, J. Lewiner, and C. Alquié, IEEE Trans. Dielectr. Electr. Insul. **5**, 2 (1998).
[6] J. M. Fourmigué, N. Verdiereand, A. Deloof, J. Berdala, and P. Dejean, in *Proceedings of the 4th International Conference on Insulated Power Cables* (SEE, Paris, 1995), pp. 231–235.
[7] C. Alquié, G. Charpak, and J. Lewiner, J. Phys. (France) Lett. **43**, 687 (1982).
[8] U. Rengel in *Proceedings of the 4th International Conference on Insulated Power Cables* (Ref. 6), pp. 175–178.
[9] Y. Li, J. Kawai, Y. Ebinuma, Y. Imaizumi, K. Suzuki, Y. Tanaka, and T. Takada, in *Proceedings of the 9th International Symposium on Electrets*, edited by Z. Xia and H. Zhang (IEEE, Piscataway, NJ, 1996), pp. 217–222.
[10] X. Qin, K. Suzuki, Y. Tanaka, and T. Takada, J. Phys. D **32**, 156 (1999).
[11] Y. Zhu and T. Takada, IEEE Trans. Dielectr. Electr. Insul. **4**, 748 (1997).
[12] A. Üstündağ, T. J. Gung, and M. Zahn, IEEE Trans. Dielectr. Electr. Insul. **5**, 421 (1998).
[13] S. Holé, T. Ditchi, and J. Lewiner, Phys. Rev. B **61**, 13 528 (2000), this reference contains two misprints: in Eq. (21) B_k should be E_k and in Eq. (47) ϵ_j should be ξ_j.
[14] O. Paris, J. Lewiner, T. Ditchi, and S. Holé, in *Proceedings of the 10th International Symposium on Electrets*, edited by A. A. Konsta, A. Vassilikou-Dova, and K. Vartzeli-Nikaki (IEEE, Piscataway, NJ, 1999), pp. 39–42.
[15] O. Paris, J. Lewiner, T. Ditchi, S. Holé, and C. Alquié, IEEE Trans. Dielectr. Electr. Insul. **7**, 556 (2000).
[16] T. Ditchi, C. Alquié, and J. Lewiner, J. Acoust. Soc. Am. **94**, 3061 (1993).
[17] P. M. Morse and K. U. Ingard, *Theoretical Acoustics* (McGraw-Hill, New York, 1968).